

Title: Rapid in situ assessment of radiocesium wood contamination using field gamma-ray spectroscopy to optimise felling.

Authors: Adam Varley¹, Andrew Tyler¹, Maksim Kudzin³, Viachaslau Zabrotski³, Justin Brown², Taras Bobrovskiy² and Mark Dowdall².

Affiliations:

¹Department of Biological and Environmental Sciences, University of Stirling, Stirling FK9 4LA, United Kingdom

²Norwegian Radiation Protection Authority, Grini næringspark 13, 1332 Østerås, Norway

³Polessie State Radiation-Ecological Reserve, Tereshkovoy Street 7, Khoyniki, Gomel Region, Belarus

Corresponding author's email address: a.l.varley@stir.ac.uk

Accepted refereed manuscript of:

Varley A, Tyler A, Kudzin M, Zabrotski V, Brown J, Bobrovskiy T & Dowdall M (2020) Rapid in situ assessment of radiocesium wood contamination using field gamma-ray spectroscopy to optimise felling. *Journal of Environmental Radioactivity*, 218, Art. No.: 106259. DOI:

<https://doi.org/10.1016/j.jenvrad.2020.106259>

© 2020, Elsevier. Licensed under the Creative Commons Attribution-NonCommercial-NoDerivatives 4.0 International <http://creativecommons.org/licenses/by-nc-nd/4.0/>

Highlights:

- Characterising caesium contamination in wood is one of the principal issues
- Current methods are inefficient leading to large volumes of waste.
- In situ and mobile gamma-ray spectrometry offer a means of real-time characterisation

Abstract

The Chernobyl nuclear power meltdown that took place in 1986 has left a radioactive contamination legacy that currently severely limits the economic potential of impacted regions including the Polessie State Radioecology Reserve in Southern Belarus. Extensive areas of forested land could potentially become economically viable for firewood and building materials if radioactive contamination, notably ^{137}Cs , could be characterised faster, whilst closely adhering to regulatory limits. Currently, laboursome tree coring and unreliable transfer factors derived from limited soil sampling data are routinely employed in felling decision making, which has financial repercussions owed to the large amounts of waste produced and unnecessary transportation costs. In this study, it is demonstrated that a combination of targeted mobile gamma-ray spectrometry and a newly developed, lead shielded, *in situ* gamma-ray spectrometry method can significantly speed up the process of characterisation of ^{137}Cs wood activity in the field. For the *in situ* method, Monte Carlo calibration routines were developed alongside spectral processing procedures to unfold spectra collected in the field allowing for separation of ground and tree spectral components. Isolated contributions from the tree could then be converted to activity. The method was validated at a test facility and then demonstrated at three separate sites with differing contamination levels. This technique showed that single trees could be measured within approximately 20 % of the activity compared to conventional tree core data. However, some discrepancies were found which were attributed to under sampling using the tree corer and low count rates at the lowest activity site, prompting the need for further data collection to optimise the method. It was concluded that this real-time approach could be a valuable tool for management of contaminated forested areas, releasing valuable timber and ultimately reducing the risk associated with living and working in these areas.

1 **1. Introduction**

2 The Chernobyl accident of April 1986 resulted in the world's largest nuclear disaster, wide
3 scale radioactive contamination being spread over much of Northern Europe with the highest
4 deposition of contamination occurring over large areas of the former USSR countries
5 encompassing modern day Russia, Belarus and Ukraine (IAEA, 2008). Areas in close
6 proximity of the nuclear power plant were particularly impacted leading to evacuation. Large
7 tracts of forested land exist in these regions which are intrinsically linked to efforts towards
8 socio-economic revitalisation of the impacted areas. The most contaminated regions in Belarus
9 occur in the southern reaches of the Gomel Region, along the border with the Ukraine. The
10 Belarusian exclusion zone functions as a scientific reserve, the Polessie State Radiation-
11 Ecological Reserve (PSRER), which covers some 216 thousand hectares. The PSRER is
12 located in a subzone of foliar (deciduous and broad-leaved) and pine woods, with forested areas
13 constituting 109.7 thousand hectares (51.1 % of the territory). Pine woods comprise 43.9 % of
14 the afforested areas, birch woods 30.7 %, black alder 12.4 %, oak 6.3 % and other species 6.7
15 %. The territories not covered by forest (primarily abandoned agricultural lands) are 82.2
16 thousand hectares (38.0 %) and non-agricultural unforested lands occupy 20.1 thousand
17 hectares (9.3 %) (Izrael et al., 1996).

18

19 Until recent years, the management of Chernobyl contaminated land, inclusive of the PSRER,
20 has been primarily oriented towards reducing external and internal doses to the public and
21 mitigating the risks for further dispersal of contaminants through natural events such as
22 forestfires or wildfires (Dvornik et al., 2018; Evangelidou, 2015). Irrespective of the radiological
23 challenges posed by contamination for forestry workers or residents of forested areas, there are
24 still direct and indirect economic impacts imposed due to radioactive contamination of forests
25 (Yoshihara et al., 2014). This is primarily in relation to regulatory limits imposed on wood and
26 wood products and their effects on the development of forestry resources (Shaw et al., 2001).
27 The important role of forestry and derived products in the current and future Belarusian
28 economy is well established (Gerasimov and Karjalainen, 2010). The area of Belarus with the
29 most forest coverage is the Gomel region and some 2 million ha (21 % of the forest fund area)
30 continues to be impacted by contamination derived from Chernobyl (Woodfuels Program,
31 2009). Wood harvesting is prohibited in areas with contamination densities in excess of 1.4
32 MBq m⁻². Relevant regulatory limits for Belarus are displayed in Table 1.

33

34 Table 1. National admissible levels for the ^{137}Cs content of timber, timber goods and other
 35 non-food forestry products in Belarus (RDU/LH-2001, 2001)

Product/Material	^{137}Cs , Bq/kg
Roundwood for construction of the walls of residential housing	740
Other roundwood products	1480
Process wood	1480
Fuel wood	740
Lumber, wooden goods and construction components (internal) for residential housing	740
Lumber, wooden goods and components, other	1850
Other inedible products	1850

36

37 Until recently, the assessment of ^{137}Cs content in contaminated forest stands has largely been
 38 based on transfer factors (TF; $\text{Bq kg}^{-1}/\text{Bq m}^{-2}$) that are based on comparing the ^{137}Cs
 39 concentration in a given tree component (Bq kg^{-1}) to the total ^{137}Cs contamination density of
 40 the soil (Bq m^{-2}) (Nimis, 1996). Many TF models have been developed using various different
 41 radionuclide, tree and soil types and have been widely used to assess the redistribution of ^{137}Cs
 42 in forest ecosystems (Ipatyev et al., 1999) and to develop broad-scale maps of forest
 43 contamination from ^{137}Cs deposition inventories (Goor and Avila, 2003; van der Perk et al.,
 44 2004). In terms of building up a general picture of wood activity across a region, TF are a
 45 practical solution given that they can be derived within a relatively short time frame either
 46 through direct soil sampling or using pre-existing decay-corrected soil activity data, combined
 47 with soil composition and land cover maps. However, predictions on a smaller scale, which
 48 are more relevant to the forestry industry, such as over tens of meters, are far more difficult
 49 owing to the environment being innately heterogeneous in terms of soil, tree type and
 50 contamination distribution. Small scale variation in contamination distribution is particularly
 51 important, as more recent studies have demonstrated that orders of magnitude of change can
 52 be observed in areas closer to the Chernobyl nuclear power plant (Golosov, 2003; Golosov et
 53 al., 2000; Adam Varley et al., 2017; Vitaly et al., 2019, 2018). In part this variation is due to

54 remobilisation, but mainly it is down to finer scale deposition patterns dictated by localised
55 meteorological events in 1986 (Varley et al., 2018). Therefore, basing wood activities for an
56 entire forest stand from TR derived from limited soil samples leaves a study particularly
57 vulnerable to very large uncertainties on final estimates.

58 The social and economic role of forestry and its products and potential future commercial
59 development of contaminated forestry areas necessitates a means of reliably and efficiently
60 assessing the ^{137}Cs content of trees. Sampling of trees by coring followed by laboratory analysis
61 is inefficient due to the number of trees involved and the time and resources required for
62 sampling and analysis prior to felling. Similarly, alternative methods based on TF's operated
63 over large areas can be unreliable potentially misclassifying large areas of otherwise productive
64 forest stand whilst still requiring analysis of potentially unrepresentative soil samples.

65 The ability to reliably estimate the ^{137}Cs level in the wood of a tree, in real-time, without the
66 need to fell a tree provides a potentially valuable tool for the forestry industry in areas that are
67 affected by radioactive contamination. Such a tool would significantly reduce waste as trees
68 can be screened prior to felling to ensure compliance with regulatory limits and harvesting
69 effort and resources can be more efficiently applied. In this context, the in situ measurement of
70 ^{137}Cs in standing trees may offer potential benefits.

71 *1.1. Field gamma-ray spectrometry of ^{137}Cs*

72 Conventionally, in situ measurements serve to establish the ^{137}Cs activity deposition (Bq m^{-2})
73 in the underlying soil and utilise the number of counts in the photopeak at 662 keV (Tyler,
74 2008). Signal contributions from other environmental media, for example trees, are typically
75 assumed to be negligible or constant, although attempts have been made at characterising
76 contributions from tree trunks and the canopy (Cresswell et al., 2016; Gering et al., 2002). For
77 measurements of the soil activity, a single measurement can be made to derive spatially
78 integrated activity estimates with appropriate correction, from soil core data or estimated from
79 inherent spectral features such as the peak-to-valley ratio (Östlund et al., 2015), for vertical
80 depth distribution of ^{137}Cs (Miller et al., 1990).

81 However, the use of in situ gamma spectrometry cannot be applied in determining the activity
82 present in a tree by simply placing a detector against the tree as there are almost always two
83 significant signal components: (i) from the contaminants in the tree; and (ii) from the

84 contaminants in ground. Untangling the signal is unfeasible as contributions from both (i) and
85 (ii) can change significantly on both spatial and temporal scales depending on the amount of
86 ^{137}Cs originally deposited, the properties of the soil and the age and species of the tree (Fogh
87 and Andersson, 2001). In addition, the primary component of the gamma photon signal in the
88 detector would be nuisance signal from the ground as the volume of soil within the field of
89 view of the detector is much larger compared to volume of the tree within the same field of
90 view (Gering et al., 2002). Furthermore, activities in the ground are orders of magnitude higher
91 due to low uptake by the tree from the ground.

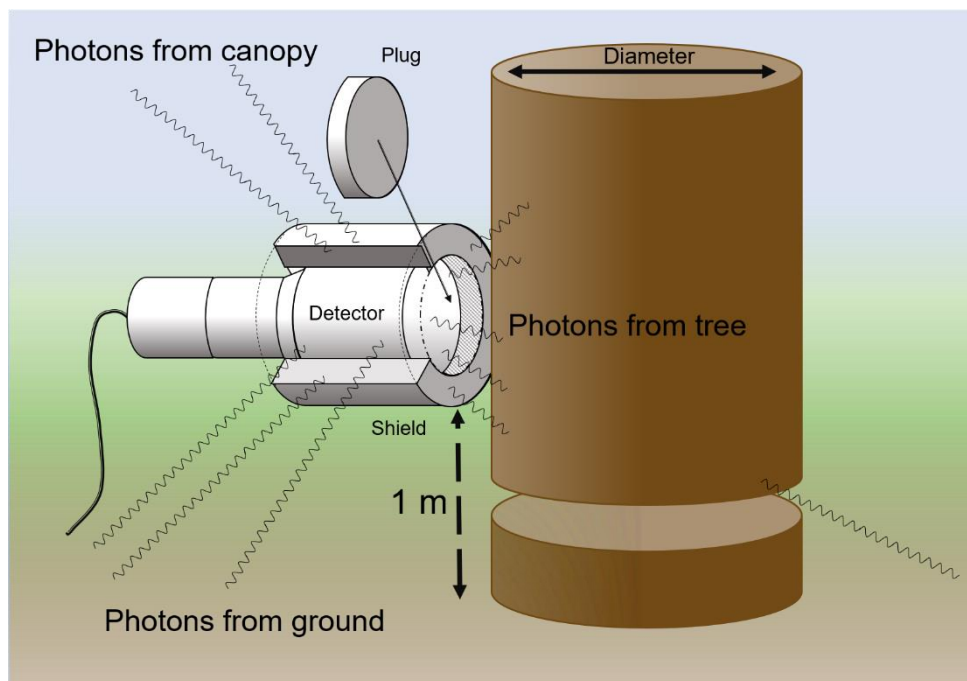
92 The next step is to take two or more separate measurements and try to separate the individual
93 components of the signal using mathematical techniques. This study explores an approach
94 employing strategically placed lead shielding around and in front of the detector to collimate
95 the signal from the tree, thus reducing background signal and canopy signal and ultimately
96 increasing the signal to noise ratio. Crucially, this setup ensures the detector remains in a
97 constant position, negating any issues associated with changes in background and wood
98 heterogeneity. In the past, a similar technique has been adopted with in situ gamma-ray
99 spectrometry, wherein lead shielding was used to collimate the detector's field of view to assess
100 the ^{137}Cs depth distribution (Benke and Kearfott, 2002). The depth of burial was also estimated
101 by using a faceplate to change the angular response of the detector to the source (Feng et al.,
102 2012).

103 The aim of this study was to develop a system that can quickly estimate the ^{137}Cs concentration
104 within the wood of the tree for a more efficient means of identifying trees that could be felled
105 for economic exploitation and reduce the need for intrusive sampling. The approach utilises
106 Monte Carlo simulations to model the gamma photon spectra to identify the optimal geometries
107 and shielding requirements for differing thicknesses of the tree and distribution of ^{137}Cs
108 throughout a tree trunk. Calibration factors were derived from simulations alongside the
109 development of regular algebraic solutions to allow careful separation of ground and tree
110 contributions. The approach to estimate ^{137}Cs activity is validated from samples taken of trees
111 measured using the shielded detector.

112 **2. Methods**

113 *2.1. Measurement procedure and spectral processing*

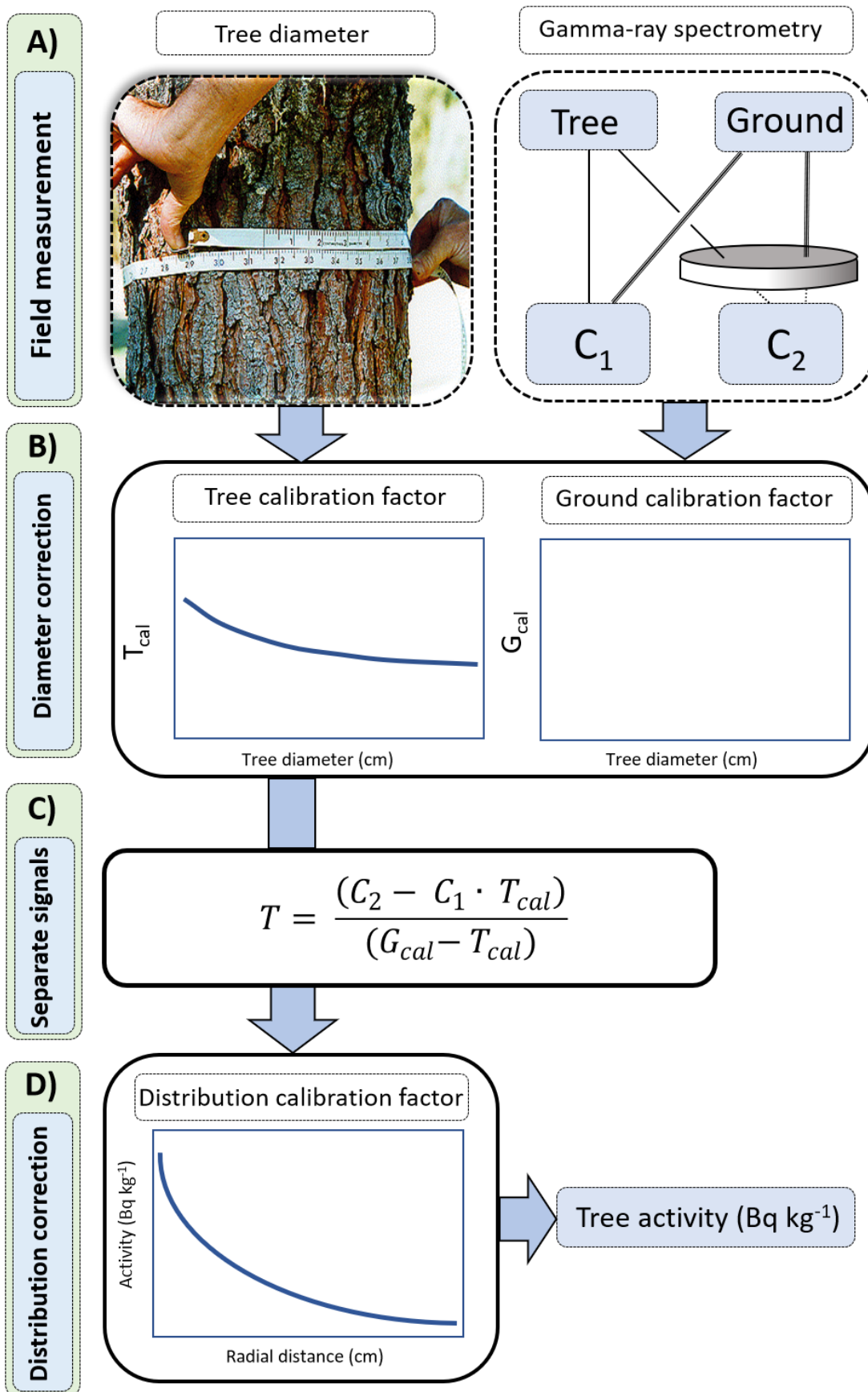
114 The first step in the measurement process involves measuring the circumference of the tree to
115 be used in the calculation of calibration coefficients to account for its diameter (Graphical
116 abstract - A). The sodium iodide detector is then fastened to the tree trunk at a height of a 1 m
117 and the first measurement is taken with the lead shield open (without the front face plug),
118 exposing the tree to the detector, the face of which is positioned 2 cm back from the front of
119 the lead collimator (Figure 1).



120

121 Figure 1. Schematic drawing of the detector, lead collimator and plug.

122 This measurement produces the count rate C_1 ; referred to as the unshielded measurement,
123 which is made up of counts derived from the ground (G) and Tree (T) (Eq. 1). The second
124 measurement is made when the plug is placed in the collimator and aims to eliminate as much
125 of the tree signal as possible and the resultant signal can be considered as a background (Figure
126 2A). Nevertheless, significant contributions from both ground and tree will still be observed in
127 the count rate (C_2) that need to be characterised using separate ground and tree calibration
128 coefficients, G_{cal} and T_{cal} , respectively (Eq. 2).



129

130 Figure 2. Flow diagram describing the in situ measurement of ^{137}Cs

131

$$C_1 = G + T \quad (1)$$

132

$$C_2 = G \cdot G_{cal} + T \cdot T_{cal} \quad (2)$$

133 Derivation of calibration coefficients is performed in the second step and account for the
134 shielding effect of the tree and plug (Figure 2B). The shielding effect from the plug is relatively
135 constant yet changes in tree diameter will have two effects on the number of photons in both
136 C_1 and C_2 (eq. 1 and 2). Photons coming from the tree will generally increase with increasing
137 tree diameter, given that there is more source volume contributing photons although the source
138 distance will be larger for photons from the edges of the tree. At the same time, counts coming
139 from the ground will generally decrease with increasing thickness as the tree will be providing
140 more shielding for photons coming from behind the tree. Acting in combination, these two
141 effects are likely to have a nonlinear relationship with tree diameter. Consequently, the
142 relationship between the ratio of shielded and unshielded counts must be characterised in
143 sufficient detail across a range of diameters forming two calibration coefficients G_{cal} and T_{cal}
144 where G_{cal} is the ratio between unshielded (G_U) and shielded (G_S) ground counts, and T_{cal} is the
145 ratio between unshielded (T_U) and shielded (T_S) tree counts described in equation's 3 and 4,
146 respectively. Essentially, each calibration coefficient is a fraction of the unshielded count.

147

$$G_{cal} = \frac{G_U}{G_S} \quad (3)$$

148

$$T_{cal} = \frac{T_U}{T_S} \quad (4)$$

149 In the third stage, equations (1) and (2) can be combined and rearranged allowing for separation
150 of the tree signal (T) (eq. 5) (Figure 2C). T represents the number of counts received by the
151 detector, originating from the tree in the unshielded measurement and can be converted into
152 activity using Monte Carlo simulations.

153

$$T = \frac{(C_2 - C_1 \cdot T_{cal})}{(G_{cal} - T_{cal})} \quad (5)$$

154 Prior to this crucial step, a correction factor must be applied to T to account for the radial
 155 distribution in the tree (Figure 2D). The observed radial distribution within a tree is due to a
 156 number of factors including deposition rates and soil type (Soukhova et al., 2003), although
 157 the primary driving force is believed to be due to the biological mobility of radiocaesium within
 158 wood, which is dependent on the species and age of the tree. In general, accumulation of
 159 caesium tends to occur in the bark and newer growth close to the phloem through which
 160 nutrients are transported to the roots. Contrastingly, lower concentrations are found in the pith
 161 and older wood towards the centre where water is transferred up to the crown and into the
 162 leaves. Importantly, differences in radial distribution can significantly influence the count rate
 163 received by the detector and considerable caution must be applied during the application of any
 164 correction factors.

$$A = P + (A_0 - P)e^{-cd} \quad (6)$$

165 From information gained from field observations, and literature values, a simplified model
 166 described by an exponential function was used to model caesium radial distribution to correct
 167 count rate to activity (Eq. 6). Activity (A) was predicted at radial depth (d) reducing according
 168 to the decay constant (c), where A_0 is the activity of the outer layer of bark and P is the activity
 169 in the pith. A visual example of a radial distribution is provided in Figure 2 in the
 170 supplementary materials using values of 1.5 and 0.1 for c and P , respectively. Although this
 171 distribution would suggest that contributions from the bark would have a significant effect on
 172 the count rate, it has been calculated that less than 4 % of the counts originate from the bark
 173 for this distribution. For larger diameters it is significantly less than 4 %. Importantly, even
 174 though the bark is closer to the detector, its relatively small mass contributes relatively little to
 175 the overall count rate compared to the rest of the tree.

176 2.2. Monte Carlo simulations

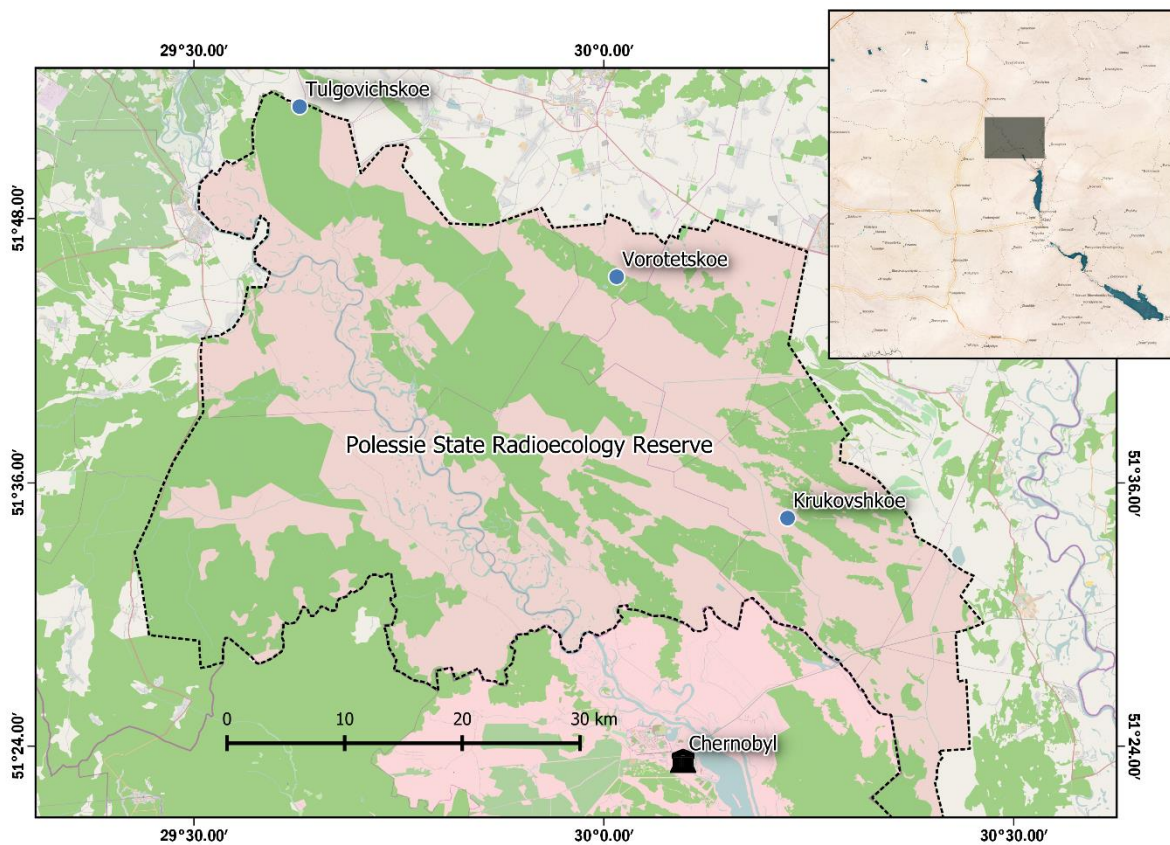
177 Calibration of the detector was performed using Monte Carlo simulations, which allowed for
 178 complex parameters such as tree diameter and radial distribution to be changed that would
 179 otherwise be unfeasible to do so through traditional analytical calibration procedures. A

180 detailed description of the modelling stage, including geometry specifications and processing
181 routines can be found in the supplementary materials.

182 *2.3. Field sites and measurement*

183 To test the approach, three field sites were selected within the PSRER in the Gomel region of
184 Belarus. The areas were specifically chosen as they covered a broad range of caesium
185 depositions. The chosen three locations were Tulgovichskoe (low activity), Vorotetskoe
186 (medium activity) and Krukovskoe (high activity). Locations of the three sites relative to the
187 Chernobyl NPP are shown in Figure 3 with further details provided in Table 2 supplementary
188 materials; based on five soil samples and corresponding dose rate measurements at each site.

189



190

191 Figure 3. Three test sites relative to the Chernobyl NPP. The dashed line indicates the boundary
192 of the Polessie Radiation Ecology Reserve.

193

194 The Tulgovichskoe site was being actively logged as the stands at the site were deemed to be
195 under the relevant regulatory limits (Table 1), whereas the Vorotetskoe and Krukovskoe sites
196 had been untouched since 1986 as they were considered near to or over Belarussian statutory
197 limits with respect to ^{137}Cs content (740 Bq kg^{-1}). A rectangular area (approximately 30×30
198 m) in which the dose rate was deemed to be the most stable spatially was identified at each of
199 the three forestry sites. The spatial distribution of ^{137}Cs was mapped at each site using a $76 \times$
200 76 mm NaI:Tl detector integrated with a high accuracy DGPS which provided reliable accuracy
201 under trees for 30 minutes once a signal had been attained. Individual spectra were converted
202 to ^{137}Cs inventory by following the procedure outlined in Varley et al. (2017).

203 Within the selected mapped areas, 10 mature trees were randomly chosen to test the in situ
204 method and a subset of 4 trees was randomly selected for wood and bark sampling prior to the
205 in situ gamma-ray measurement. Trees were randomly selected by randomly generating
206 coordinates in the map and selecting the closest tree to that coordinate. Wood samples were
207 taken with a tree corer (Haglöf, 5.15 mm diameter, length 300 mm). The remaining 6 trees
208 were not physically sampled, but in situ measurements were performed. Three trees from the
209 Vorotetskoe and Krukovskoe sites were felled to serve as test logs: one pine (*Pinus sylvestris*)
210 from Vorotetskoe, one pine from Krukovskoe and one birch (*Betula pendula*) from
211 Vorotetskoe. The felled trees were moved to an unforested area of low ^{137}Cs activity ($\sim 333 \text{ Bq}$
212 kg^{-1}) producing negligible counts from the background. This area was referred to as the test
213 facility. Samples were taken from tests logs from the duramen (dead, central heartwood) and
214 the alburnum (the living secondary sapwood) using a chainsaw alongside bark samples taken
215 with an axe. Samples of each of these three materials were then analysed by HPGe in the
216 laboratory for ^{137}Cs content.

217 In situ measurements were taken with an InspectorTM 1000 from Canberra and count times
218 were of the order of 3 – 5 minutes, typically resulting in a counting uncertainty under the full
219 energy peak at 661 keV of below 2%.

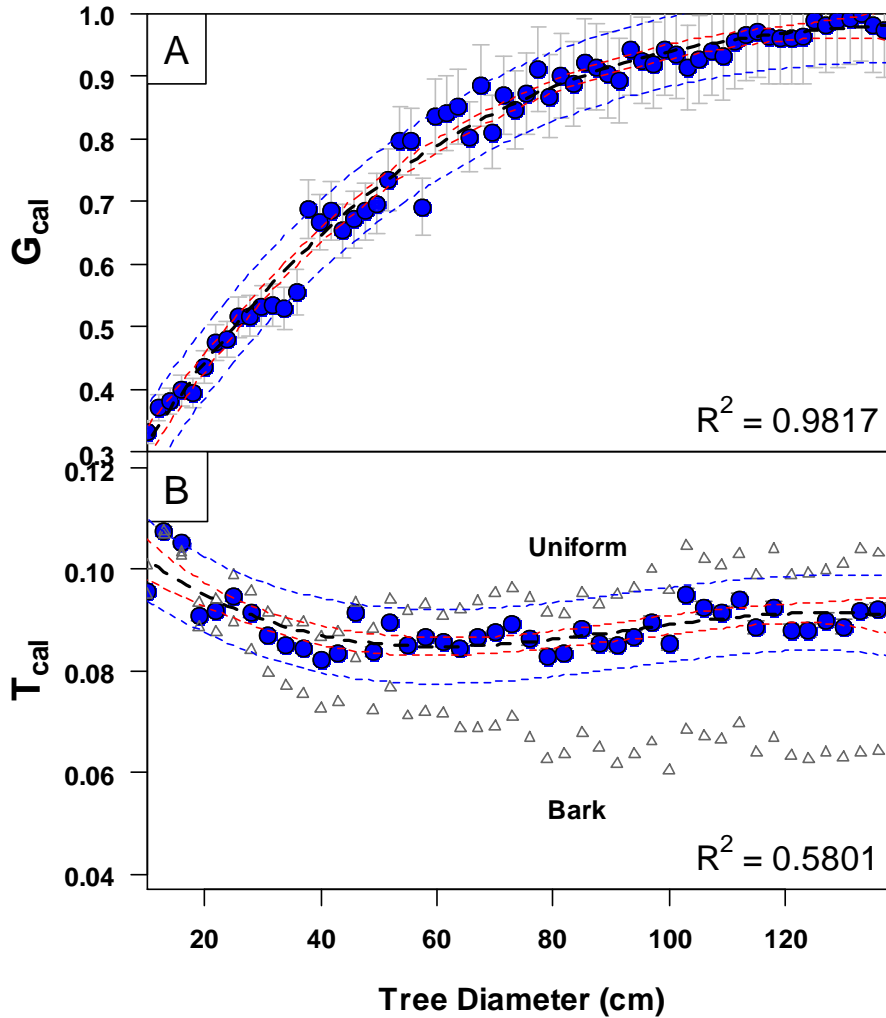
220 3. Results and Discussion

221 3.1. Monte Carlo results

222 Tree and ground results derived from Monte Carlo give insight into how the detection system
223 interacts with the shield, plug, ground and tree (Figure 4). For the ground model changes in
224 tree diameter effectively introduce shielding and this can be realised as a gradual decrease in
225 the number of counts entering through the front face of the detector in the unshielded (G_U)
226 measurement. Concurrently, this has less of an effect on the shielded measurement (G_S) as it is
227 already partially shielded by the plug. Acting in combination to produce the value G_{cal} , the ratio
228 between G_U and G_S effectively enters a state of equilibrium ($G_{cal} = 1$) at around 120 cm, as this
229 thickness of the tree effectively shields all photon coming from the front face (Figure 4A).
230 Across a typical tree diameter range, G_{cal} can vary by up to 70 %. Importantly, it is this
231 relationship that allows the method to work and for the signal to be separated. The diameter of
232 the tree can be inputted into the model and for a certain diameter of tree, the drop in count rate
233 can be predicted from G_{cal} leaving the tree count rate.

234 It is a different case for T_{cal} , where the influence of the tree diameter has very little effect on the
235 ratio between unshielded (T_U) and shielded (T_S) measurements, where only minor variations in
236 T_{cal} are witnessed (8 - 10 %) across the diameter range (Figure 4B). Notice that the radial
237 distribution can have a slight influence on T_{cal} , for example the difference between a uniform
238 and a distribution mostly associated with the bark. Yet, in terms of potential uncertainty, this is
239 low in comparison to the final calibration stage in Eq 6, where large variations in radial depth
240 distribution could introduce orders of magnitude of change in the count rate for the same overall
241 activity.

242



243

244 Figure 4. Model fits derived from Monte Carlo data for ground (A) and tree (B) calibration
 245 factors, G_{cal} and T_{cal} , as a function of tree diameter. Fitted polynomial models display both
 246 confidence (red broken lines) and prediction (blue lines) intervals at 95% and error bars
 247 represent counting uncertainty (1σ). Triangles show the influence of tree diamtere on T_{cal} when
 248 ^{137}Cs is either distributed uniformly throughout the trunk or located predominantly in the bark.

249 3.2. Test logs

250 To test the performance of the detector and shield within a relatively controlled environment,
 251 measurements were taken from three test logs (taken from high activity areas) over relatively
 252 low activity ground. In this scenario, the count rate from the log was many orders of magnitude
 253 higher than the background. These controlled conditions allowed Monte Carlo results derived
 254 purely for the tree to be assessed without significant contribution from the ground and
 255 importantly provide verification for the distribution model.

256 Observing the ratio between duramen (heartwood) and alburnum (sapwood) ¹³⁷Cs
 257 concentrations in wood tissue between the pine logs and birch logs confirmed that the trees
 258 have different radial distributions, but still contain higher contamination towards the outside of
 259 the tree in the living wood and the bark (Table 4 in supplementary material). By analysing the
 260 duramen/alburnum ratio it becomes clear that contamination within pine species (0.442-0.482)
 261 tends to be closer to the bark of the tree compared to the birch tree (1.080-1.230) (Table 2).
 262 This finding matches general patterns found by other studies on distributions of this isotope in
 263 trees (Ohashi et al., 2014; Soukhova et al., 2003). The limited sample size was not enough to
 264 draw significant conclusion on radial distribution but was enough to approximately
 265 parameterise Monte Carlo models to derive activity estimates from in situ count rates.

266 Table 2. Cs-137 activity concentrations in various radial sections of the test logs based on
 267 laboratory measurement. Measurement uncertainties 2σ for laboratory and *in situ*
 268 measurements.

Test log	Average wood activity (Bq kg ⁻¹)	In situ estimate (Bq kg ⁻¹)	Duramen/alburnum activity concentration ratio
Pine (Krukovskoe) – base of log	4220 ± 1200	4260 ± 1350	0.442
Pine (Krukovskoe) – top of log	5170 ± 1460	5200 ± 1800	0.456
Pine (Vorotetskoe) – base of log	841 ± 249	816 ± 315	0.482
Pine (Vorotetskoe) – top of log	619 ± 182	664 ± 249	0.454
Birch (Vorotetskoe) – base of log	551 ± 157	716 ± 283	1.080
Birch(Vorotetskoe) – top of log	452 ± 131	507 ± 205	1.230

269 Laboratory results from wood samples taken from the test facility were compared to
 270 measurements made along the logs using the in situ detector (Table 2). In situ measurements
 271 were calibrated using the conservative parameters from the radial distribution data for the pine
 272 test logs. It was decided that due to the potentially more complex distribution within the birch
 273 trees, and the smaller amount of data available, the pine distribution would be fitted to the birch
 274 tree results. Furthermore, the pine distribution was more relevant to this study as most of the
 275 trees that were measured in the field were Scots Pine trees.

276 Wood samples and in situ activity estimates were within 7 % of each other for the test pine logs.
 277 Wood activity estimates for the birch log were less reliable (< 25 %), this is understandable
 278 given that the exponential radial distribution that was fitted to the pine data will be different
 279 compared to that of a typical birch radial distribution (Table 2).

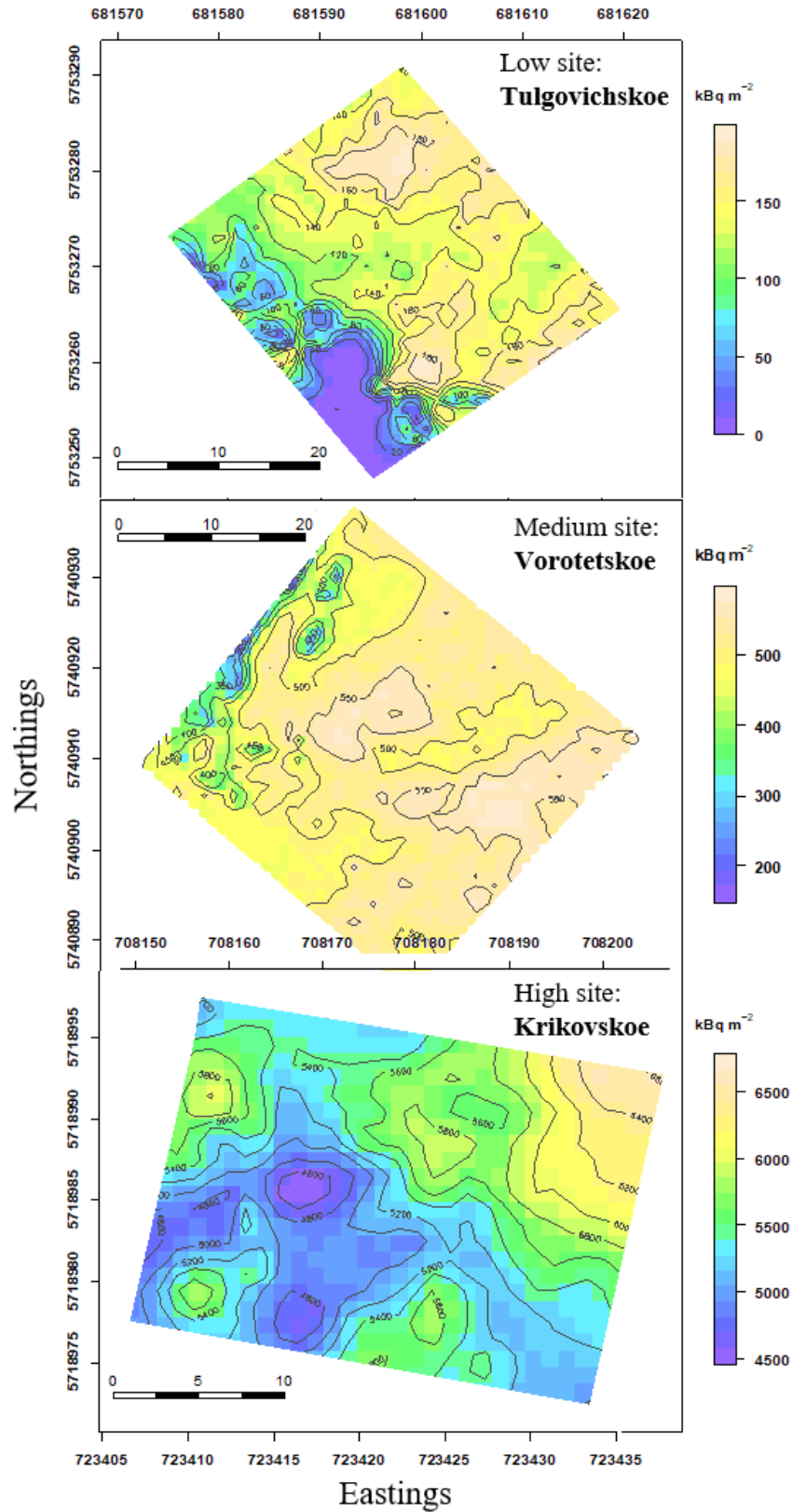
280 3.3. *Soil transfer factors*

281 As discussed earlier, the conventional way of estimating activity levels in trees is by use of
282 concentration ratios. A statistical summary of ^{137}Cs concentration ratios for various groups of
283 relevance to this study is shown in Table S2 in the supplementary materials which was extracted
284 from IAEA (2014).

285 The most suitable values to apply were from the category ‘Trees: broad-leaf’ for birch and
286 ‘Trees coniferous’ for pine, albeit that essentially identical concentration ratios are provided for
287 both categories. The underlying datasets used to derive transfer factors are generally considered
288 to be characterised by log-normal distributions (Sheppard, 2005) and thus the geometric mean
289 provides the most appropriate selection for a best estimate or central tendency of the CR value
290 (see Table S3 in the supplementary materials).

291 3.4. *Field site deposition patterns*

292 Although site selection aimed to find 3 areas that were relatively spatially uniform, mapped by
293 mobile gamma-ray spectroscopy results, indicate that there was considerable heterogeneity
294 across all 3 sites Figure 5 . This is not a surprising result given that across much of the exclusion
295 zone contamination tends to be heterogeneous and can be difficult to characterise without
296 equipment such as a mobile gamma-ray spectrometry operating a spatially sensitive differential
297 GPS. Although not displayed, little difference in ^{137}Cs depth distribution, derived using the
298 peak-to-valley ratio, was found within each site. Between sites there was also not a significant
299 difference in depth. Most of the contamination was estimated to be within the top 10 cm of the
300 soil surface



301

302 Figure 5. Spatial distribution of ^{137}Cs at each of the three sites chosen for the study.

303 The capability to map contamination at high spatial resolution raises potential issues in using
304 transfer factor approaches that rely on a small amount of soil samples to statistically derive soil
305 activity. At each of the three sites, clearly issues could be encountered using a limited soil
306 sampling size within a heterogeneous environment. In this scenario, the true value of mobile
307 gamma-ray spectrometry becomes clear, as these measurements by themselves could quite
308 easily be used to inform transfer factors and provide a rapid means of characterising forest
309 stands. After which measurements could be used to target the in situ method on specific trees.

310 3.5. *Wood activity estimates*

311 In general, good agreement is seen between in situ wood activity estimates (Bq kg^{-1}) and wood
312 activities taken using coring device (Table 3). In particular ID 1-5, taken at the high activity
313 site (Krukovskoe) shows a deviation of less than 20 % with exception of ID 3 (~50 % deviation).
314 This high level of agreement could be attributed to the diameter of the trees being relatively
315 small and being relatively consistent across the site. Not only did this make in situ
316 measurements easier and the modelling process more straightforward, but the corer could reach
317 closer to the centre of the tree providing a representative sample of wood throughout the radial
318 distribution and would result in more consistency between trees. Furthermore, a low counting
319 uncertainty could be achieved in a relatively short amount of time due to the high levels of
320 contamination.

321 Trees that were measured using the *in situ* detector, but did not have corresponding wood
322 sample data, still adhered closely to wood activity estimates from nearby trees for which wood
323 sample data was available suggesting that wood activity was reasonably consistent across the
324 site (3200-5330 Bq kg^{-1}). The variability present at this site is, interestingly, comparable to the
325 variability shown across the site from that identified using mobile gamma-ray spectrometry
326 (Table 5 in the supplementary materials). GPS coordinates taken in the field to mark trees were
327 accrued using a standard GPS without differential correction and were not reliable enough to
328 allow for direct comparison.

329 Activities estimated from the medium activity site (Vorotetskoe) were for the most part
330 reflective of wood sampling estimates (~20 %) for IDs 12-14. In situ estimates for ID 15 were
331 considerably different to the wood estimate (>55 %). This disparity could be caused by the trees
332 especially large diameter meaning that the 300 mm coring device probably significantly under
333 sampled the middle of the tree taking relatively more of the higher activity wood present in the

334 sapwood. Examination of the rest of the in situ measurements without matching wood sample
335 data tends to support this argument as many of the predicted wood activities were between 382-
336 529 Bq kg⁻¹ (Table 3).

337 The least comparable results were found at the lowest activity site. Notice that the in situ
338 estimate (125 ± 44 Bq kg⁻¹) for ID 21 is over 2 times that of the wood estimate (54 ± 12 Bq kg⁻¹).
339 However, these results were proved not to be significantly different using a one-way
340 ANOVA. Interestingly this was the only birch tree measured in the field and, in concurrence
341 with the test logs, an overestimate of activity was found. This is most likely a consequence of
342 the model being inappropriate for the birch tree radial distribution as it was fitted to pine tree
343 data. However, further deviations of 100 % were found for the remaining two pine trees,
344 although these were not found to be significantly different. These results are harder to explain
345 as the wood sample estimates are lower than the in situ estimates, which cannot be explained
346 by the larger diameters of the trees such as the case at the medium site. Ascertaining the exact
347 reason for this outcome is difficult, although perhaps the low count rates at this site played a
348 significant role and increased uncertainty. Another possibility is that the radial distribution
349 could have been considerably different at this site as is the forest stand was visually very
350 different and contained a greater diversity of trees and had a different soil type. It is evident that
351 further research is required to resolve this issue.

352 Estimates made using the TR method were fairly robust in terms of encapsulating the maximum
353 and minimum bounds of the wood sampled activity estimates and the in situ and mobile gamma-
354 ray spectrometry activity estimates. It is understandable why TR are widely adopted
355 particularly if there are only soil activity estimates available.

356

357

358

359

360

361

362

363

364 Table 3. Wood activity at field sites derived from wood cores, in situ measurements and
 365 transfer factors. Measurement uncertainties are quoted to 2σ .

Site	ID	Tree circumference (cm)	Species	Core samples	In situ	Transfer factor
				Wood activity (Bq kg ⁻¹)	Wood activity (Bq kg ⁻¹)	Wood activity (Bq kg ⁻¹)
Krukovskoe	1	141	Pine	3410 ± 705	3310 ± 1050	2040 – 6350
Krukovskoe	2	122	Pine	3200 ± 680	3930 ± 1270	2040 – 6350
Krukovskoe	3	122	Pine	3200 ± 680	4900 ± 1610	2040 – 6350
Krukovskoe	4	96	Pine	4010 ± 840	4490 ± 1550	2040 – 6350
Krukovskoe	5	82	Pine	3600 ± 750	4280 ± 1452	2040 – 6350
Krukovskoe	6	117	Pine	-	4160 ± 1400	2040 – 6350
Krukovskoe	7	118	Pine	-	3270 ± 1200	2040 – 6350
Krukovskoe	8	138	Pine	-	3200 ± 1010	2040 – 6350
Krukovskoe	9	119	Pine	-	4110 ± 1370	2040 – 6350
Krukovskoe	10	87	Pine	-	5330 ± 2010	2040 – 6350
Krukovskoe	11	120	Pine	-	3670 ± 1220	2040 – 6350
Vorotetskoe	12	114	Pine	578 ± 123	521 ± 177	260 - 545
Vorotetskoe	13	169	Pine	575 ± 125	463 ± 162	260 - 545
Vorotetskoe	14	169	Pine	575 ± 125	445 ± 156	260 - 545
Vorotetskoe	15	178	Pine	1010 ± 209	435 ± 158	260 - 545
Vorotetskoe	16	114	Pine	-	593 ± 201	260 - 545
Vorotetskoe	17	111	Pine	-	417 ± 143	260 - 545
Vorotetskoe	18	112	Pine	-	382 ± 131	260 - 545
Vorotetskoe	19	89	Pine	-	518 ± 194	260 - 545
Vorotetskoe	20	99	Pine	-	529 ± 190	260 - 545
Tulgovichskoe	21	110	Birch	54 ± 12	125 ± 44	60 - 112
Tulgovichskoe	22	152	Pine	48 ± 11	96 ± 29	60 - 112
Tulgovichskoe	23	152	Pine	48 ± 11	94 ± 29	60 - 112
Tulgovichskoe	24	213	Pine	67 ± 16	70 ± 19	60 - 112
Tulgovichskoe	25	211	Oak	-	87 ± 23	60 - 112
Tulgovichskoe	26	185	Pine	-	65 ± 18	60 - 112
Tulgovichskoe	27	169	Pine	-	76 ± 23	60 - 112

Matched data are displayed in bold

366 3.6. Future directions

367 It is clear from the findings of this study that being able to rapidly measure activity activity
 368 concentrations of ¹³⁷Cs across the site and in wood using non-destructive *in situ* gamma-ray
 369 spectrometry represents a considerable step forward in characterising contaminated forests such

370 as those found in the Polessie State Radioecology Reserve. The methods capability could
371 certainly become a useful prospecting tool for the forestry industry that could improve decision
372 making as to whether a tree should be felled or not depending on specified regulatory limits.
373 Such an approach might conceivably comprise two phases: (i) in situ or mobile mapping the
374 understory soil contamination levels to highlight likely areas for felling followed by
375 (ii) measurements of tree activity for verification through in situ measurements coupled with a
376 subset of trees being subject to laboratory measurement validation.

377 The outstanding uncertainties identified by this study were found to be the radial distribution
378 of the contaminant within trees of different species and wood density, which were modelled
379 from preliminary field and literature observations. Understanding how these environmental
380 parameters drive the observed count rate of the system is the next crucial step. For example,
381 accurate characterisation of green wood density is necessary for each individual measurement,
382 although this could be feasibly determined in field using tree cores or modelled using historical
383 data.

384 Perhaps a more demanding challenge is to reliably account for changes in radial distribution.
385 To accomplish this, large amounts of empirical data will have to be acquired to investigate
386 patterns in the shape of the radial distribution for a given species considering the age and
387 diameter of the tree and perhaps the underlying soil distribution. Current estimates from the
388 models developed in this study suggest that without confident resolution of this parameter final
389 wood activity estimates could be orders of magnitude from the true value and no better than
390 estimates of transfer factors, albeit without the need for physical sampling. Although
391 discrepancies between *in situ* and coring estimates were not found to be to this level within this
392 study, differences at the low activity site could in part be explained by this occurrence.

393 A final argument for the further development of this *in situ* method is the unpredictability of
394 the core data taken during this study. The results suggest that *in situ* results could in fact be
395 more representative of the true activity value, by showing less statistical variation, than the core
396 values that were used to validate due to the consistency in results displayed across each site.

397 It must be noted, ^{137}Cs poses less risk to human health compared with ^{90}Sr with regards to wood
398 contamination as strontium is absorbed more readily by trees. However, ^{90}Sr is more difficult
399 to measure in situ as it does not have a significant gamma-ray emission, therefore is only
400 feasible to measure through laboratory equipment.

401 **4. Conclusions**

402 A non-destructive in situ gamma spectrometric method to measure ^{137}Cs contamination in trees
403 has been described and demonstrated in a forest in the Belarusian Chernobyl exclusion zone.
404 The real-time method showed promising agreement with wood activity estimates made using a
405 traditional tree coring device and laboratory gamma-ray spectrometry. Potentially, the method
406 could be widely adopted, alongside mobile gamma-ray spectrometry, negating the need for a
407 tree to be felled and prolonged laboratory measurement of sampled environmental media.
408 Wider investigations into the uncertainties distributions associated with wood density and radial
409 distribution are required. Larger scale datasets are required to parameterise the underlying
410 models used to separate the signal from the tree and the background and the final radial
411 distribution calibration factor to derive wood activity.

412 **Acknowledgements**

413 The authors are grateful to the workers of the scientific part of the Polesie State Radiation
414 Ecology Reserve: V. Kalinin, E. Kalyhan, N. Dzemenkavets, A. Masheuski, N. Blinova, A.
415 Uhljanets and D. Garbaruk for fieldwork, sample preparation and laboratory analysis.

416

417

418

419

420

421

422 **5. References**

- 423 Auty, D., Achim, A., Macdonald, E., Cameron, A.D., Gardiner, B.A., 2014. Models for
424 predicting wood density variation in Scots pine. *Forestry* 87, 449–458.
425 <https://doi.org/10.1093/forestry/cpu005>
- 426 Beck, H., DeCampo, J., Gogolak, C., 1972. In situ Ge(Li) and NaI(Tl) gamma-ray spectrometry.
427 New York. <https://doi.org/10.2172/4599415>
- 428 Benke, R.R., Kearfott, K.J., 2002. Demonstration of a collimated in situ method for determining
429 depth distributions using g-ray spectrometry, *Nuclear Instruments and Methods in Physics*
430 *Research A*.
- 431 Briesmeister, J.F., 1993. MCNP-A general Monte Carlo N-particle transport code. LA-12625.
- 432 Cresswell, A.J., Kato, H., Onda, Y., Nanba, K., 2016. Evaluation of forest decontamination
433 using radiometric measurements. *J. Environ. Radioact.* 164, 133–144.
434 <https://doi.org/10.1016/j.jenvrad.2016.07.024>
- 435 de Groot, A. V., van der Graaf, E.R., de Meijer, R.J., Maučec, M., 2009. Sensitivity of in-situ
436 γ -ray spectra to soil density and water content. *Nucl. Instruments Methods Phys. Res. Sect.*
437 *A Accel. Spectrometers, Detect. Assoc. Equip.* 600, 519–523.
438 <https://doi.org/10.1016/j.nima.2008.12.003>
- 439 Dvornik, A.A., Dvornik, A.M., Korol, R.A., Shamal, N. V., Gaponenko, S.O., Bardyukova, A.
440 V., 2018. Potential threat to human health during forest fires in the Belarusian exclusion
441 zone. *Aerosol Sci. Technol.* 52, 923–932.
442 <https://doi.org/10.1080/02786826.2018.1482408>
- 443 Evangeliou, N., 2015. Fire evolution in the radioactive forests of Ukraine and Belarus: future
444 risks for the population and the environment. *Ecol. Monogr.* 85, 49–72.
- 445 Feng, T.C., Jia, M.Y., Feng, Y.J., 2012. Method-sensitivity of in-situ gamma spectrometry to
446 determine the depth-distribution of anthropogenic radionuclides in soil. *Nucl. Instruments*
447 *Methods Phys. Res. Sect. A-Accelerators Spectrometers Detect. Assoc. Equip.* 661, 26–
448 30. <https://doi.org/10.1016/j.nima.2011.09.014>

449 Fogh, C.L., Andersson, K.G., 2001. Dynamic behaviour of ¹³⁷Cs contamination in trees of the
450 Briansk region, Russia. *Sci. Total Environ.* 269, 105–115. <https://doi.org/10.1016/S0048->
451 9697(00)00819-6

452 Gerasimov, Y., Karjalainen, Y., 2010. (PDF) Atlas of the forest sector in Belarus. Work. Pap.
453 Finnish For. Res. Inst. 170Publisher Finnish For.

454 Gering, C.F., Kiefer, P., Fesenko, S., Voigt, G., 2002. In situ gamma-ray spectrometry in
455 forests: determination of kerma rate in air from. *J. Environ. Radioact.* 61, 75–89.

456 Golosov, V., 2003. Application of Chernobyl-derived ¹³⁷Cs for the assessment of soil
457 redistribution within a cultivated field. *Soil Tillage Res.* <https://doi.org/10.1016/S0167->
458 1987(02)00130-7

459 Golosov, V.N.V., Walling, D., Kvasnikova, E.V.E., Stukin, E.D., Nikolaev, A.N., Panin, A. V.,
460 2000. Application of a field-portable scintillation detector for studying the distribution of
461 ¹³⁷Cs inventories in a small basin in Central Russia. *J. Environ. Radioact.* 48, 79–94.
462 [https://doi.org/10.1016/S0265-931X\(99\)00058-2](https://doi.org/10.1016/S0265-931X(99)00058-2)

463 Goor, F., Avila, R., 2003. Quantitative comparison of models of ¹³⁷Cs cycling in forest
464 ecosystems. *Environ. Model. Softw.* 18, 273–279. <https://doi.org/10.1016/S1364->
465 8152(02)00075-0

466 Goor, F., Davydchuk, V., Vandenhove, H., 2003. GIS-based methodology for Chernobyl
467 contaminated land management through biomass conversion into energy - A case study
468 for Polessie, Ukraine. *Biomass and Bioenergy* 25, 409–421.
469 [https://doi.org/10.1016/S0961-9534\(03\)00034-5](https://doi.org/10.1016/S0961-9534(03)00034-5)

470 Goor, F., Thiry, Y., 2004. Processes, dynamics and modelling of radiocaesium cycling in a
471 chronosequence of Chernobyl-contaminated Scots pine (*Pinus sylvestris* L.) plantations.
472 *Sci. Total Environ.* 325, 163–180. <https://doi.org/10.1016/j.scitotenv.2003.10.037>

473 Harrison, R.L., 2009. Introduction to Monte Carlo simulation, in: *AIP Conference Proceedings*.
474 pp. 17–21. <https://doi.org/10.1063/1.3295638>

475 IAEA, 2008. Environmental consequences of the Chernobyl accident and their remediation: 20
476 years of experience. *Chernobyl.* <https://doi.org/10.1093/rpd/ncl163>

- 477 Ipatyev, V., Bulavik, I., Baginsky, V., Goncharenko, G., Dvornik, A., 1999. Forest and
478 Chernobyl: Forest ecosystems after the Chernobyl nuclear power plant accident: 1986-
479 1994. *J. Environ. Radioact.* 42, 9–38. [https://doi.org/10.1016/S0265-931X\(98\)00042-3](https://doi.org/10.1016/S0265-931X(98)00042-3)
- 480 Izrael, Y.A., De Cort, M., Jones, A.R., Nazarov, I.M., Fridman, S.D., Kvasnikova, E. V., Stukin,
481 E.D., Kelly, G.N., Matveenکو, I.I., Pokumeiko, Y.M., Tabatchnyi, L.Y., Tsaturon, Y.,
482 1996. The atlas of caesium-137 contamination of Europe after the Chernobyl accident.
483 *Radiol. consequences Chernobyl Accid.* 1–10.
- 484 Kirk, B.L., 2010. Overview of Monte Carlo radiation transport codes, in: *Radiation*
485 *Measurements*. Pergamon, pp. 1318–1322. <https://doi.org/10.1016/j.radmeas.2010.05.037>
- 486 Likar, A., Vidmar, T., Lipoglavsek, M., Omahen, G., 2004. Monte Carlo calculation of entire
487 in situ gamma-ray spectra. *J. Environ. Radioact.* 72, 163–168.
- 488 Malins, A., Okumura, M., Machida, M., Takemiya, H., Saito, K., 2015. Fields of View for
489 *Environmental Radioactivity* 2–7.
- 490 Maučec, M., De Meijer, R.J., Van Der Klis, M.M.I.P., Hendriks, P.H.G.M., Jones, D.G., 2004.
491 Detection of radioactive particles offshore by gamma-ray spectrometry Part II: Monte
492 Carlo assessment of acquisition times. *Nucl. Instruments Methods Phys. Res. Sect. A*
493 *Accel. Spectrometers, Detect. Assoc. Equip.* 525, 610–622.
494 <https://doi.org/10.1016/j.nima.2004.01.075>
- 495 Maučec, M., Hendriks, P.H.G.M., Limburg, J., de Meijer, R.J., 2009. Determination of
496 correction factors for borehole natural gamma-ray measurements by Monte Carlo
497 simulations. *Nucl. Instruments Methods Phys. Res. Sect. A Accel. Spectrometers, Detect.*
498 *Assoc. Equip.* 609, 194–204. <https://doi.org/http://dx.doi.org/10.1016/j.nima.2009.08.054>
- 499 Melin, J., Wallberg, L., Suomela, J., 1994. Distribution and retention of cesium and strontium
500 in Swedish boreal forest ecosystems. *Sci. Total Environ.* 157, 93–105.
501 [https://doi.org/10.1016/0048-9697\(94\)90568-1](https://doi.org/10.1016/0048-9697(94)90568-1)
- 502 Miller, K.M., Kuiper, J.L., Helfer, I.K., 1990. ¹³⁷Cs fallout depth distributions in forest versus
503 field sites: Implications for external gamma dose rates. *J. Environ. Radioact.* 12, 23–47.
504 [https://doi.org/10.1016/0265-931X\(90\)90034-S](https://doi.org/10.1016/0265-931X(90)90034-S)

- 505 Myttenaere, C., Schell, W.R., Thiry, Y., Sombre, L., Ronneau, C., van der Stegen de Schrieck,
506 J., 1993. Modelling of Cs-137 cycling in forests: recent developments and research needed.
507 Sci. Total Environ. 136, 77–91. [https://doi.org/http://dx.doi.org/10.1016/0048-](https://doi.org/http://dx.doi.org/10.1016/0048-9697(93)90298-K)
508 9697(93)90298-K
- 509 Narayan, R.D., Miranda, R., Rez, P., 2012. Monte Carlo simulation for the electron cascade
510 due to gamma rays in semiconductor radiation detectors. J. Appl. Phys. 111, 64910.
511 <https://doi.org/10.1063/1.3698370>
- 512 Nimis, P.L., 1996. RADIOCESIUM IN PLANTS OF FOREST ECOSYSTEMS, Studia
513 Geobotanica.
- 514 Ohashi, S., Okada, N., Tanaka, A., Nakai, W., Takano, S., 2014. Radial and vertical
515 distributions of radiocesium in tree stems of *Pinus densiflora* and *Quercus serrata* 1.5 y
516 after the Fukushima nuclear disaster. J. Environ. Radioact. 134, 54–60.
517 <https://doi.org/10.1016/j.jenvrad.2014.03.001>
- 518 Östlund, K., Samuelsson, C., Rääf, C.L., 2015. Experimentally determined vs: Monte Carlo
519 simulated peak-to-valley ratios for a well-characterised n-type HPGe detector. Appl.
520 Radiat. Isot. <https://doi.org/10.1016/j.apradiso.2014.09.022>
- 521 RDU/LH-2001, 2001. Republican permissible levels of content of ¹³⁷Cs in wood, products
522 from wood and wood materials and other non-edible products of forestry (in Russian).
- 523 Shaw, G., Robinson, C., Holm, E., Frissel, M.J., Crick, M., 2001. A cost-benefit analysis of
524 long-term management options for forests following contamination with ¹³⁷Cs. J.
525 Environ. Radioact. 56, 185–208. [https://doi.org/10.1016/S0265-931X\(01\)00053-4](https://doi.org/10.1016/S0265-931X(01)00053-4)
- 526 Sheppard, S.C., 2005. Transfer parameters-Are on-site data really better? Hum. Ecol. Risk
527 Assess. <https://doi.org/10.1080/10807030500257747>
- 528 Soukhova, N. V, Fesenko, S. V, Klein, D., Spiridonov, S.I., Sanzharova, N.I., Badot, P.M.,
529 2003. Cs distribution among annual rings of different tree species contaminated after the
530 Chernobyl accident, Journal of Environmental Radioactivity.
- 531 Strandgard, M., Walsh, D., 2011. Improving harvester estimates of bark thickness for radiata
532 pine (*Pinus radiata* D.Don). South. For. a J. For. Sci. 73, 101–108.

- 533 <https://doi.org/10.2989/20702620.2011.610876>
- 534 Thiessen, K.M., Thorne, M.C., Maul, P.R., Pröhl, G., Wheater, H.S., 1999. Modelling
535 radionuclide distribution and transport in the environment, in: *Environmental Pollution*.
536 Elsevier Science Ltd, pp. 151–177. [https://doi.org/10.1016/S0269-7491\(99\)00090-1](https://doi.org/10.1016/S0269-7491(99)00090-1)
- 537 Thiry, Y., Garcia-Sanchez, L., Hurtevent, P., 2015. Experimental quantification of radiocesium
538 recycling in a coniferous tree after aerial contamination: Field loss dynamics, translocation
539 and final partitioning. *J. Environ. Radioact.* 161, 42–50.
540 <https://doi.org/10.1016/j.jenvrad.2015.12.017>
- 541 Thiry, Y., Goor, F., Riesen, T., 2002. The true distribution and accumulation of radiocaesium
542 in stem of Scots pine (*Pinus sylvestris* L.). *J. Environ. Radioact.* 58, 243–259.
543 [https://doi.org/10.1016/S0265-931X\(01\)00068-6](https://doi.org/10.1016/S0265-931X(01)00068-6)
- 544 Tyler, A.N., 2008. In situ and airborne gamma-ray spectrometry, in: *Radioactivity in the*
545 *Environment, Analysis of Environmental Radionuclides*. Elsevier, pp. 407–448.
546 [https://doi.org/10.1016/S1569-4860\(07\)11013-5](https://doi.org/10.1016/S1569-4860(07)11013-5)
- 547 van der Perk, M., Burema, J., Vandenhove, H., Goor, F., Timofeyev, S., 2004. Spatial
548 assessment of the economic feasibility of short rotation coppice on radioactively
549 contaminated land in Belarus, Ukraine, and Russia. I. model description and scenario
550 analysis. *J. Environ. Manage.* 72, 217–232.
551 <https://doi.org/10.1016/j.jenvman.2004.05.002>
- 552 Varley, A., Tyler, A., Bondar, Y., Hosseini, A., Zabrotski, V., Dowdall, M., 2018.
553 Reconstructing the deposition environment and long-term fate of Chernobyl ¹³⁷Cs at the
554 floodplain scale through mobile gamma spectrometry. *Environ. Pollut.* 240, 191–199.
555 <https://doi.org/10.1016/J.ENVPOL.2018.04.112>
- 556 Varley, Adam, Tyler, A., Dowdall, M., Bondar, Y., Zabrotski, V., 2017. An in situ method for
557 the high resolution mapping of ¹³⁷Cs and estimation of vertical depth penetration in a
558 highly contaminated environment. *Sci. Total Environ.* 605–606, 957–966.
559 <https://doi.org/10.1016/j.scitotenv.2017.06.067>
- 560 Varley, A., Tyler, A., Dowdall, M., Bondar, Y., Zabrotski, V., 2017. An in situ method for the

561 high resolution mapping of¹³⁷Cs and estimation of vertical depth penetration in a highly
562 contaminated environment. Sci. Total Environ. 605–606.
563 <https://doi.org/10.1016/j.scitotenv.2017.06.067>

564 Vitaly, L., Sokolov, A., Saveliev, A.A., 2019. Spatial analysis and modeling of cesium-137
565 redistribution in the soil cover of the Bryansk region Spatial analysis and modeling of
566 cesium-137 redistribution in the soil cover of the Bryansk region, in: EGU General
567 Assembly 2019At: Viena, Austria.

568 Vitaly, L., Sokolov, A., Saveliev, A.A., Mironenko, I. V, 2018. Landscape-scale modelling to
569 predict soil lateral migration using Cs-137 on the Bryansk Opolje region (Russia) In :
570 GlobalSoilMap Digital Soil Mapping from Country to Globe Eds . Dom ..., in:
571 GlobalSoilMap.

572 Woodfuels Program, E., 2009. Program to set up the production of wood pellets (pellets), wood
573 briquettes and coal in the organizations of the Ministry of Forestry 2009-2011 (in Russian).

574 Yoshihara, T., Matsumura, H., Tsuzaki, M., Wakamatsu, T., Kobayashi, T., Hashida, S. nosuke,
575 Nagaoka, T., Goto, F., 2014. Changes in radiocesium contamination from fukushima in
576 foliar parts of 10 common tree species in Japan between 2011 and 2013. J. Environ.
577 Radioact. 138, 220–226. <https://doi.org/10.1016/j.jenvrad.2014.09.002>

578

579

580

581

582

583

584

585